DOI 10.1007/s10812-022-01349-x
Journal of Applied Spectroscopy, Vol. 89, No. 2, May, 2022 (Russian Original Vol. 89, No. 2, March–April, 2022)

UPCONVERSION LUMINESCENCE OF Er^{3+} IONS FROM BARIUM TITANATE XEROGEL POWDER AND TARGET FABRICATED BY EXPLOSIVE COMPACTION METHOD

N. V. Gaponenko,[a,*] L. V. Sudnik,[b] P. A. Vityaz,[b] A. R. Luchanok,[b] M. V. Stepikhova,[c] A. N. Yablonskiy,[c] E. I. Lashkovskaya,[a] K. V. Shustsikava,[a] Yu. V. Radyush,[d] V. D. Zhivulko,[d] A. V. Mudryi,[d] N. M. Kazuchits,[e] and M. S. Rusetsky[e]

UDC 535.37:546.666

Photo- and cathodoluminescence in the visible range from erbium-doped barium titanate xerogels obtained in the form of a powder and a target pressed from it by explosive compaction are investigated. The powder and target exhibit upconversion luminescence of erbium ions excited at wavelengths in the regions 950–1000 and 1450–1550 nm that is characterized by strong bands at 650 and 520–560 nm and a weak band at ~820 nm that correspond to the $^4F_{9/2} \rightarrow {}^4I_{15/2}$, $^2H_{11/2} \rightarrow {}^4I_{15/2}$, $^4S_{3/2} \rightarrow {}^4I_{15/2}$, and $^4I_{9/2} \rightarrow {}^4I_{15/2}$ transitions of Er^{3+}. The target also demonstrates cathodoluminescence at room temperature and liquid nitrogen temperature with the strongest bands at 650, 520, and 538 nm.

Keywords: *erbium, upconversion luminescence, cathodoluminescence, sol–gel, barium titanate, explosive compaction method.*

Introduction. Erbium (Er)-doped films and targets are interesting for a variety of practical problems. Er-doped films, which demonstrate population inversion of the first excited state of Er^{3+}, are used as the waveguide channel and active medium to fabricate planar waveguide amplifiers [1]. Upconversion of Er luminescence (transformation of long- into short-wavelength radiation) is interesting for visualization and detection of laser IR radiation, coatings for increasing the efficiency of solar cells by expanding the spectral sensitivity range [2, 3], and luminescent images for protecting items from counterfeiting [4]. Luminescence of Er^{3+} is studied in materials with different bandgaps, phonon energies, and optical losses, e.g., Al_2O_3; SiO_2 [5]; In_2O_3 (6]; yttrium–aluminum garnets [7]; monocrystalline, amorphous, and porous silica [8]; barium titanate [9–11]; lithium niobate [12], etc. Upconversion of Er^{3+} luminescence in barium titanate was demonstrated earlier [9–11]. Recently, upconversion of Er^{3+} luminescence in barium titanate powder with >3 at.% Er formed by sol–gel synthesis, in coatings deposited by spraying a suspension containing such powder [13], and in multilayered films of barium titanate on silica with a scattering layer of porous strontium titanate [14] was demonstrated by us.

Thin-film electrooptical modulators [15, 16], multilayered interference filters with blocking of IR radiation [17], optical microresonators with enhanced luminescence [18], photonic crystals with a retuned resonance mode [19], and other photonics structures based on barium titanate thin films have been formed. Both sol–gel synthesis of films and vacuum technologies for deposition of films from targets were used to form these structures. The sol–gel synthesis made it possible to control the component ratio in the sol and; correspondingly, in the solid-state material, i.e., the xerogel, and had a characteristically low production cost. However, the method was not used effectively enough to fabricate targets designed for subsequent sputtering and vacuum deposition of films.

*To whom correspondence should be addressed.

[a]Belarusian State University of Informatics and Radioelectronics, Minsk, Belarus; email: nik@nano.bsuir.edu.by; [b]State Scientific Institution "Powder Metallurgy Institute named after academician O. V. Roman," Minsk, Belarus; [c]Institute for Physics of Microstructures, Russian Academy of Sciences, Nizhny Novgorod, Russia; [d]Scientific-Practical Materials Research Centre, National Academy of Sciences of Belarus, Minsk, Belarus; [e]Belarusian State University, Minsk, Belarus.
Translated from Zhurnal Prikladnoi Spektroskopii, Vol. 89, No. 2, pp. 184–190, March–April, 2022. Original article submitted November 26, 2021; https://doi.org/10.47612/0514-7506-2022-89-2-184-190.

The present work demonstrated the ability to form a target from Er-doped barium titanate xerogel powder by explosive compaction and upconversion of Er^{3+} photoluminescence (PL) and cathodoluminescence in the target.

Experimental. The starting materials for forming Er-doped barium titanate xerogels were titanium isopropoxide [$Ti(OC_3H_7)_4$], barium acetate [$Ba(CH_3COO)_2$], erbium acetate hydrate [$Er(CH_3COO)_3 \cdot xH_2O$], acetylacetone ($CH_3COCH_2COCH_3$), and acetic acid ($CH_3COOH$). The amounts of titanium isopropoxide and barium acetate were chosen so that the Ti/Ba ratio corresponded to the stoichiometric composition of barium titanate in the films (Ti:Ba = 1:1). The mixture was stirred for 1 h on an electrical mechanical stirrer until all components were completely dissolved. This resulted in the formation of a stable film-forming sol. Erbium acetate hydrate was added to the fresh $BaTiO_3$ sol. The mixture was stirred until it was completely dissolved.

The sol was evaporated to produce a powder. The dry powder was heated in a drying cabinet at 200°C for 30 min. The xerogel powder was formed by further heat treatment at 1000°C for 60 min.

Targets were compacted by pulses from a planar impact wave generator. An ammonium nitrate compound with a detonation rate of ~4000 m/s was used for the compaction. The developed explosive compaction method produced a planar detonation front that allowed mixing of the upper layers to be significantly reduced and the faceting of the formed target to be improved. A target of diameter 48 mm and thickness 4 mm was formed from the $BaTiO_3$ xerogel powder. X-ray phase analysis of the samples used a DRON-3 automated diffractometer with monochromatic CuK_α-radiation. X-ray diffraction patterns were recorded at points in steps of $2\theta = 0.04^o$ and exposures of 2 s at each point. The elemental composition of the powder and target were studied by energy-dispersive microanalysis on a Hitachi-S4800 microscope equipped with an x-ray microanalysis accessory.

Upconversion of Er^{3+} luminescence in the obtained samples was excited with continuous optical pumping by focused diode-laser radiation with $\lambda = 980$ nm and power 200 mW. The wavelength of this radiation corresponded to the absorption band for the electronic transition of Er^{3+} from the $^4I_{15/2}$ ground state to the $^4I_{11/2}$ second excited state. The detector for recording upconversion luminescence in the visible range was an R9110 photomultiplier (Hamamatsu, Japan). Signals were processed using synchronous phase detection. Upconversion luminescence spectra of targets were measured both at room temperature and liquid N_2 temperature (77 K) with a fragment of the target immersed in N_2.

Upconversion PL spectra were studied with pulsed pumping. PL excitation spectra were generated using a parametric light generator (ORO, Solar-LS) excited by the third harmonic (355 nm) of YAG:Nd-laser pulsed radiation. The pulse length was 5 ns, repetition rate 10 Hz, average excitation power ~5 mW. The pump radiation wavelength was continuously retuned in the range 900–1600 nm during recording of upconversion PL excitation spectra. Upconversion luminescence in the visible range was recorded using an Acton 2300i grating monochromator, photomultiplier, and LeCroy digital oscilloscope.

Cathodoluminescence was excited at room temperature and 77 K using an electron gun with energy 10 keV and current density 0.05 mA/cm^2. Spectra were recorded using a photomultiplier in the range 200–900 nm with spectral resolution 0.2 nm [20]. A fragment of the target was attached to the cryostat copper cooling coil filled with liquid N_2 for the low-temperature measurements.

Results and Discussion. Figure 1 shows portions of x-ray diffraction patterns of starting Er-doped $BaTiO_3$ xerogel powder and a target produced by explosive compaction of it. Indices of the perovskite cubic modification are noted. However, we could not unambiguously assign these diffraction patterns to the cubic or tetragonal perovskite modification. The lines in the powder diffraction patterns were asymmetric. The intensity ratio of the 111 and 200 peaks corresponded to the peak ratio of samples with the tetragonal structure (PDF 83-1880, 89-1428) while lines 100, 200, 210, and 211 had the expected bulging to the left in the tetragonal structure that was indicative of tetragonal distortion of the powder crystal lattice. Thus, the parameters of the tetragonal cell could not be evaluated.

The diffraction lines of the explosively compacted sample were slightly shifted to smaller angles and broadened. The half-widths at half-height of lines 100, 110, 111, and 200 were 0.25, 0.24, 0.20, and 0.34, respectively. Lines 110 and 111 unique for the tetragonal modification had half-widths at half-height comparable to those of the other lines. This could be indicative of both the cubic modification of $BaTiO_3$ and the tetragonal modification with slightly different *a* and *c* constants. The lattice parameters calculated in the cubic form were 4.005 and 4.015 Å for the powder and target. The powder of the formed xerogel had a grainy structure with a grain size of ~0.1–0.2 μm (Fig. 2).

Energy-dispersive analysis of the powder and target was consistent with atomic concentrations of the target and powder atoms within the root-mean-square deviation. Table 1 lists the concentrations of Ba, C, Er, O, and Si for the powder. The Er concentration was >3 at.% in the powder and target.

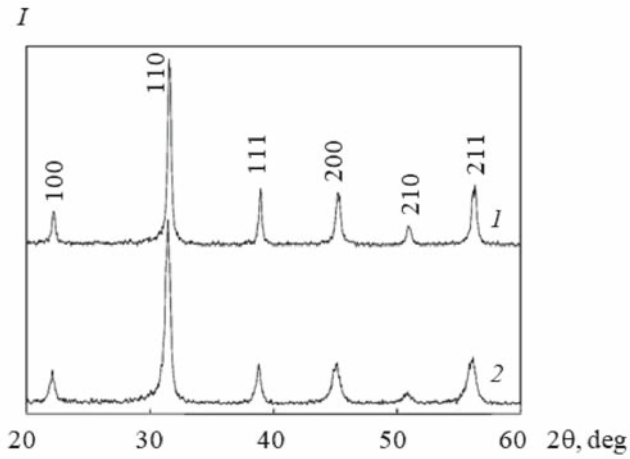

Fig. 1. Diffraction patterns of Er-doped barium titanate xerogel powder obtained from sol of composition $BaTiO_3$ (60 mg/mL) and Er_2O_3 (13.0 mg/mL) (1) and a target fabricated from this powder (2).

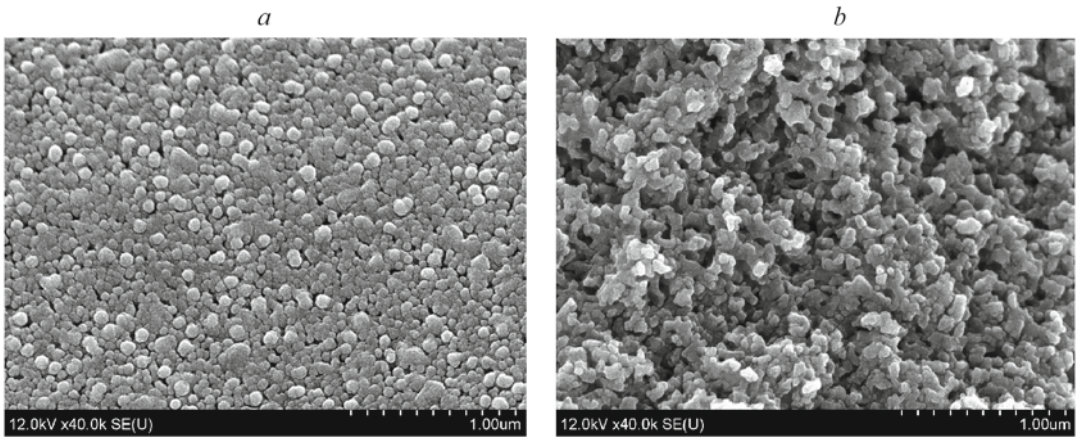

Fig. 2. SEM images of Er-doped powder (a) and target (b) of barium titanate xerogel.

TABLE 1. Average Concentrations of Elements (at.%) and Root-Mean-Square Deviations Obtained by Energy-Dispersive Microanalysis of Er-Doped Barium Titanate Xerogel Powder (Set Size 5)

Element	Average value, at.%	Root-mean-square deviation
Ba	13.46	2.25
C	10.07	3.06
Er	3.75	0.81
O	58.57	5.70
Ti	14.16	3.78

The powder and target demonstrated Er^{3+} upconversion luminescence upon excitation by continuous IR radiation with $\lambda = 980$ nm. Figure 3 shows upconversion luminescence spectra of the target. Luminescence of Er^{3+} in the $BaTiO_3$ powder and target was characterized by bands in the range 400–850 nm with the strongest bands in the range 520–560 nm and near 650 nm. The observed PL bands belonged to the $^2H_{9/2} \rightarrow {}^4I_{15/2}$, $^2H_{11/2} \rightarrow {}^4I_{15/2}$, $^4S_{3/2} \rightarrow {}^4I_{15/2}$, $^4F_{9/2} \rightarrow {}^4I_{15/2}$,

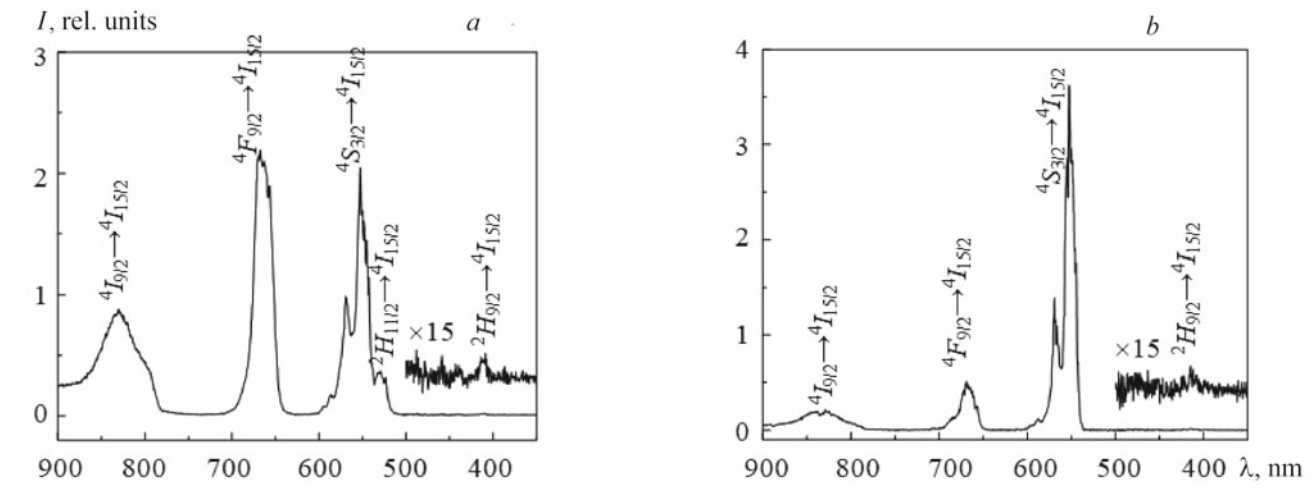

Fig. 3. Upconversion PL spectra at 300 (a) and 78 K (b) of Er^{3+} in a target pressed from barium titanate xerogel powder with excitation by continuous IR radiation at λ = 980 nm.

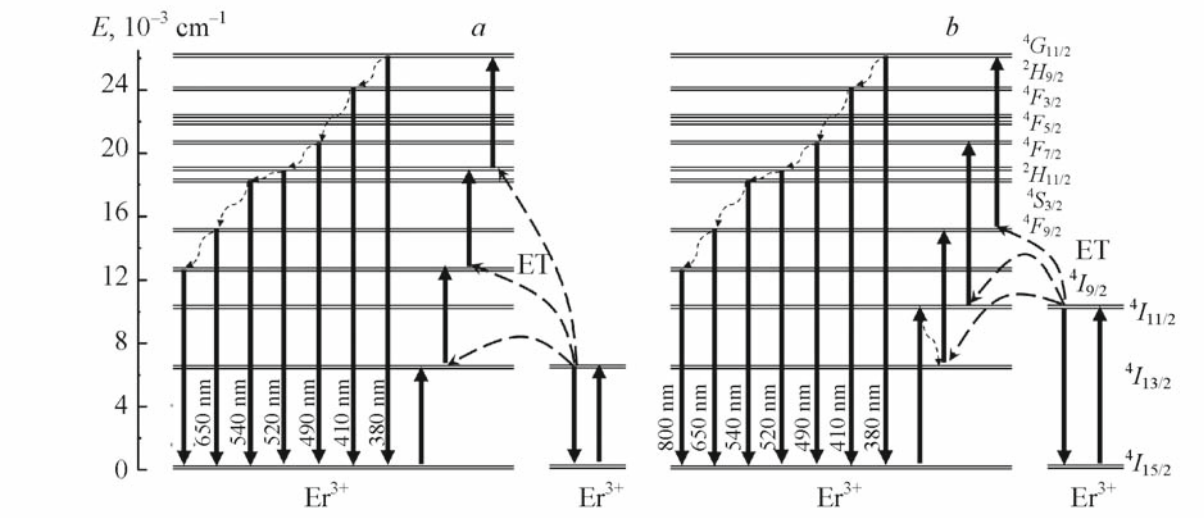

Fig. 4. Energy diagram and scheme of excitation and relaxation processes of Er^{3+} for excitation at λ_{ex} = 1500 (a) and 980 nm (b); small wavy arrows denote nonradiative relaxation of Er^{3+}; large dashed arrows, cooperative upconversion with energy transfer (ET) from one excited ion to another and conversion of the latter to a higher energy level.

and $^4I_{9/2} \rightarrow {}^4I_{15/2}$ transitions of Er^{3+}. It is noteworthy that excitation of upconversion PL was not observed under these same conditions for xerogel powder with a lower Er concentration (~1 at.%) [13]. Therefore, it could be assumed that the conversion of IR radiation into visible results from cooperative upconversion, i.e., interaction of neighboring Er^{3+} associated with energy transfer from one excited ion to another with conversion of the latter into a higher energy level (Fig. 4).

Figure 5 shows upconversion PL excitation spectra (for λ = 550 nm) in Er-doped $BaTiO_3$ xerogel powder measured in the near-IR region. Two relatively broad bands near 980 and 1530 nm that corresponded to Er^{3+} transitions from the ground ($^4I_{15/2}$) into the second ($^4I_{11/2}$) and first excited state ($^4I_{13/2}$) were observed. Thus, upconversion PL in the obtained samples could be excited via absorption of IR radiation in the ranges 960–995 and 1455–1555 nm.

The inset in Fig. 5 shows upconversion PL spectra obtained with pulsed optical excitation at λ_{ex} = 980 and 1534 nm that corresponded to maxima in the PL excitation spectra. The difference in the intensity ratio of the different bands in the upconversion PL spectra obtained with continuous and pulsed optical excitation (cf. Figs. 3 and 5, inset) could be explained by the substantially greater excitation power density for pulsed pumping. An increase in the excitation power is known to

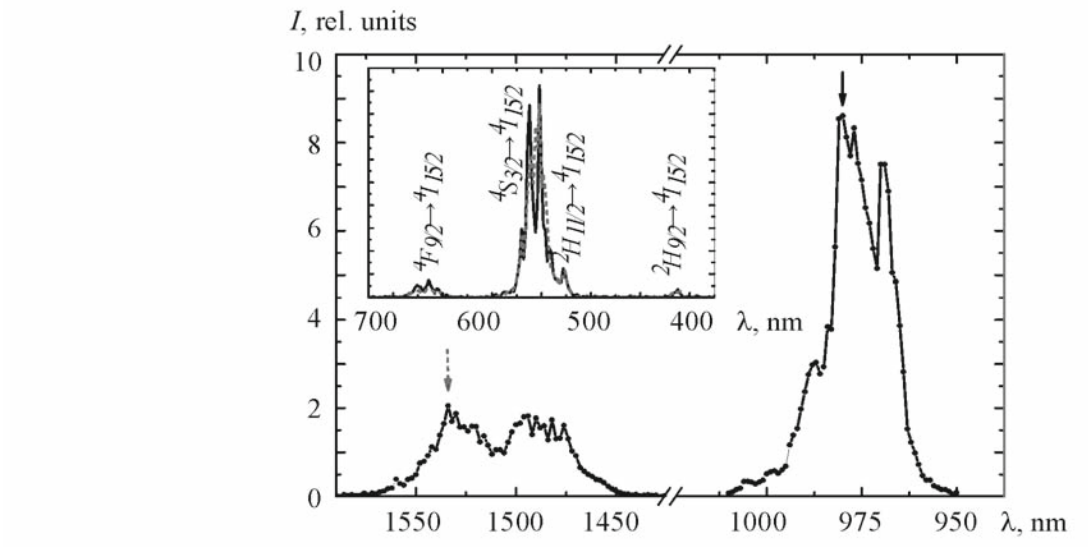

Fig. 5. Upconversion PL excitation spectrum of Er^{3+} ($\lambda = 550$ nm) in barium titanate xerogel powder in the near-IR range; pump radiation pulse length 5 ns, repetition rate 10 Hz; in the inset, normalized upconversion PL spectra with excitation by pulsed radiation at $\lambda_{ex} = 980$ and 1534 nm (denoted by arrows in the PL excitation spectrum) with an indication of the corresponding Er^{3+} emission transitions.

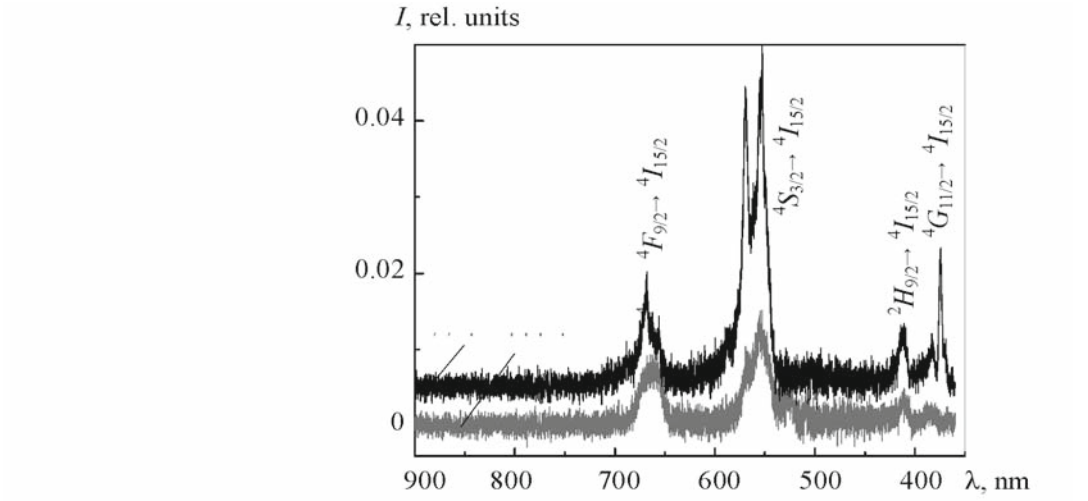

Fig. 6. Cathodoluminescence spectra of an Er^{3+}-doped barium titanate target.

lead to redistribution of intensity between red and green bands of Er^{3+} upconversion luminescence corresponding to the $^4F_{9/2} \rightarrow {}^4I_{15/2}$ and $^2H_{11/2}, {}^4S_{3/2} \rightarrow {}^4I_{15/2}$ transitions [11, 21, 22].

The target also demonstrated cathodoluminescence in the visible region at room temperature and 77 K with the strongest bands in the green range, corresponding to the $^2H_{11/2} \rightarrow {}^4I_{15/2}$ and $^4S_{3/2} \rightarrow {}^4I_{15/2}$ transitions and a weaker band, $^4F_{9/2} \rightarrow {}^4I_{15/2}$ (Fig. 6). Degradation of the target and weakening of the cathodoluminescence over time was not observed. The cathodoluminescence spectrum at 77 K exhibited an additional luminescence band with a maximum at 383 nm that belonged to the Er^{3+} $^4G_{11/2} \rightarrow {}^4I_{15/2}$ transition.

Conclusions. Sol–gel technology was adapted to the synthesis of Er-doped $BaTiO_3$ powder and a target formed from the powder by explosive compaction. Upconversion luminescence of Er in $BaTiO_3$ powder and the target was demonstrated with excitation near 980 and 1534 nm. The target demonstrated cathodoluminescence of Er in the visible region in addition

to upconversion luminescence. Considering the interest in $BaTiO_3$ films, the proposed method for forming an Er-doped $BaTiO_3$ target could be used for vacuum sputtering and formation of microresonator components, optical filters, planar waveguides, and luminescent coatings [23].

Acknowledgments. The work was supported by a joint grant of the Russian Foundation for Basic Research and the Belarusian Republican Foundation for Fundamental Research (RFBR 20-52-00039 Bel_a, BRFBR X203-388).

REFERENCES

1. J. D. B. Bradley and M. Pollnau, *Laser Photonics Rev.*, **5**, No. 3, 368–403 (2011).
2. A. Shalav, B. S. Richards, and M. A. Green, *Sol. Energy Mater. Sol. Cells*, **1**, No. 9, 829–842 (2007).
3. J. C. Goldschmidt and S. Fischer, *Adv. Opt. Mater.*, **3**, No. 11, 1487–1497 (2015).
4. L. Liu, D. Yan, L. Xu, Z. Zhou, X. Sun, Y. Liu, X. Zong, E. Zhao, J. Ren, J. Zhang, and H. Li, *J. Lumin.*, **224**, 117306–117311 (2020).
5. A. Polman, *J. Appl. Phys.*, **82**, 1–39 (1997).
6. A. Podhorodecki, R. Kudrawiec, J. Misiewicz, N. V. Gaponenko, and D. A. Tsyrkunov, *Opt. Mater.*, **28**, 685–687 (2006).
7. E. Garskaite, M. Lindgren, M.-A. Einarsrud, and T. Grande, *J. Eur. Ceram. Soc.*, **30**, 1707–1715 (2010).
8. N. V. Gaponenko, *Acta Phys. Pol., A*, **112**, 737–749 (2007).
9. L. Chen, X.-h. Wei, and X. Fu, *Trans. Nonferrous Met. Soc. China*, **22**, 1156–1160 (2012).
10. A. Meneses-Franco, M. Campos-Vallette, S. Octavio Vasquez, and E. A. Soto-Bustamante, *Materials*, **11**, 1950–1961 (2018).
11. H. Bae, E. Lee, and K. T. Lee, *Phys. Chem. Chem. Phys.*, **23**, 14587–14591 (2021).
12. A. J. Kenyon, *Prog. Quantum Electron.*, **26**, 225–284 (2002).
13. N. V. Gaponenko, Yu. D. Kornilova, E. I. Lashkovskaya, V. D. Zhivul′ko, A. V. Mudryi, Yu. V. Radyush, B. A. Andreev, M. V. Stepikhova, A. N. Yablonskii, S. A. Gusev, R. Subasri, and D. S. Reddy, *Fiz. Tekh. Poluprovodn.*, **55**, No. 9, 713–718 (2021).
14. M. V. Rudenko, N. V. Gaponenko, E. B. Chubenko, E. I. Lashkovskaya, K. V. Shustsikava, Yu. V. Radyush, V. D. Zhivulko, A. V. Mudryi, M. Wang, E. V. Monaico, M. V. Stepikhova, and A. N. Yablonskiy, *J. Adv. Dielectr.*, 2150031 (2021).
15. A. Petraru, J. Schubert, M. Schmid, and Ch. Buchal, *Appl. Phys. Lett.*, **81**, No. 8, 1375–1377 (2002).
16. A. Karvounis, F. Timpu, V.V. Vogler-Neuling, R. Romolo Savo, and R. Grange, *Adv. Opt. Mater.*, **8**, 2001249–2001271 (2020).
17. R. Subasri, D. S. Reddy, K. R. C. Soma Raju, K. S. Rao, P. Kholov, and N. Gaponenko, *Res. Chem. Intermed.*, **45**, No. 8, 4179–4191 (2019).
18. N. V. Gaponenko, P. A. Kholov, T. F. Raichenok, and S. Ya. Prislopski, *Opt. Mater.*, **96**, 109265–109269 (2019).
19. N. V. Gaponenko, P. A. Kholov, Yu. D. Kornilova, E. I. Lashkovskaya, V. A. Labunov, I. L. Martynov, E. V. Osipov, A. A. Chistyakov, N. I. Kargin, T. F. Raichenok, and S. A. Tikhomirov, *Fiz. Tekh. Poluprovodn.*, **55**, No. 10, 912–915 (2021).
20. N. M. Kazuchits, M. S. Rusetsky, V. N. Kazuchits, and A. M. Zaitsev, *Diamond Relat. Mater.*, **74**, 41–44 (2017).
21. T. C. Rich and D. A. Pinnow, *J. Appl. Phys.*, **43**, 2357–2365 (1972).
22. I. A. Khodasevich, A. A. Kornienko, P. P. Pershukevich, V. A. Aseev, M. A. Khodasevich, and A. S. Grabtchikov, *J. Appl. Spectrosc.*, **84**, 986–994 (2017).
23. E. F. Schubert, A. M. Vredenberg, N. E. J. Hunt, Y. H. Wong, P. C. Becker, J. M. Poate, D. C. Jacobson, L. C. Feldman, and G. J. Zydzik, *Appl. Phys. Lett.*, **61**, 1381–1383 (1992).